Supporting Information

Harnessing secondary phases for rapid magnitude estimation with DAS offshore Chile and its implications for Early Warning

C. Strumia[1], A. Trabattoni[2], A. Scala[1], D. Rivet[2], G. Festa[1,3]

[1]Università di Napoli Federico II, Physics Department, Complesso Monte S. Angelo, Napoli, Italy.

[2]Université Côte d'Azur, Observatoire de la Côte d'Azur, CNRS, IRD, Géoazur.

[3]Istituto Nazionale di Geofisica e Vulcanologia, Osservatorio Nazionale Terremoti, Roma, Italy.

Introduction

Here we include further information that supports the results shown in the main text. Starting from showing time delays between direct P and converted P-to-S phases, we then detail amplitude properties of quantities different from displacement. Also, we add more examples of rapid magnitude estimation, also including technical details on parameters used for obtaining the results shown in the main text. Finally, we show the observed trends in amplitude amplification and site corrections estimated along the cables.

S1

Here we report the average time duration available for the estimation of the peak amplitude of the P phase. For each event the time windows adopted for the measure started 0.2s before the manual picks to account for possible picking errors, and had a fixed duration based on earthquake magnitude, as described in Text S1 and Tab S1. In case the available time window was shorter because of the onset of following arrivals, we reduced the windows duration to exclude any overlapping. The converted Ps phase generated at the sedimentary layers arrives on average within $1s$ after the first P wave recordings, reducing the available time for the measure of peak displacement. Figure S2 shows the average P wave window duration for each of the three cables, as a function of the position along the fiber.

The CCN.N cable exhibits average durations coherent with the analysis of Trabattoni et al. (2024). Moreover, this cable shows larger available time windows with respect to SER.S and SER.N cables, suggesting thicker sedimentary layers.

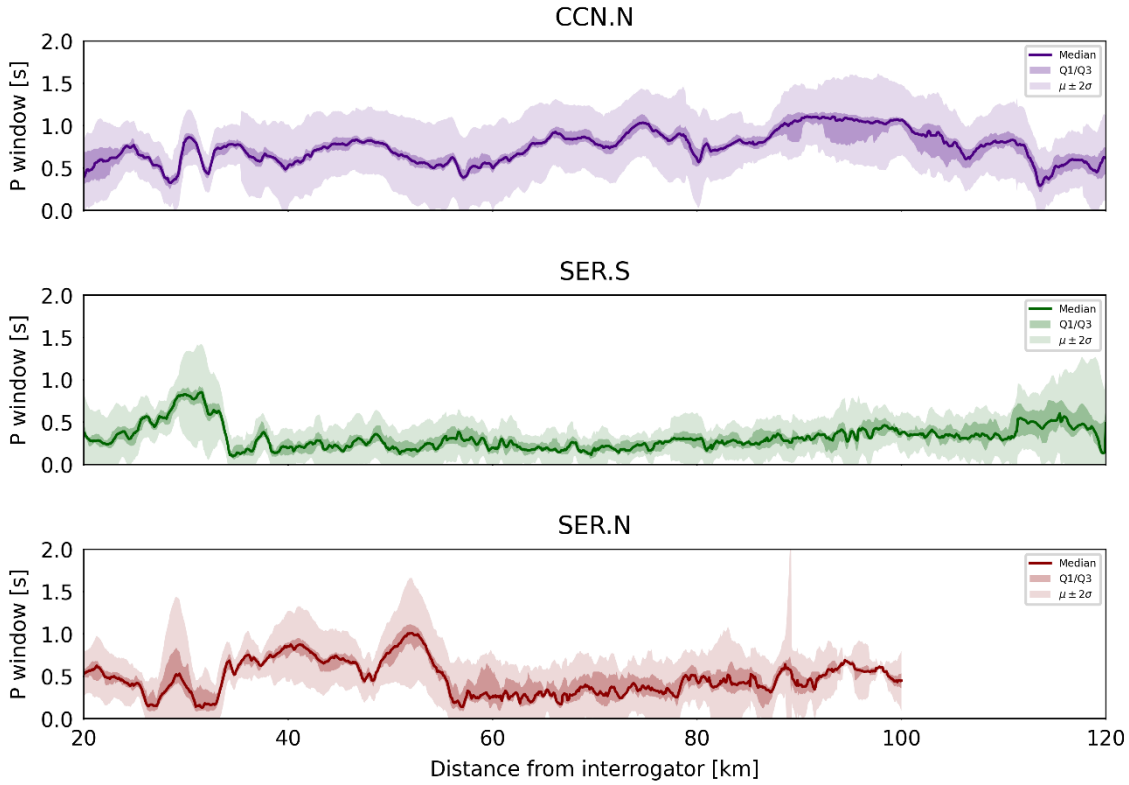

Figure S1. Time duration of P wave time window as a function of the distance along the cable, for each of the three cables. Each plot represents the median duration (solid bold lines), the first and third quantiles of the distributions (darker shaded area) and the intervals defined by twice the standard deviation (light shaded area).

S2

As described in the Methods section, we analyzed peak amplitude properties also for the strain rate and the time integral of the strain. First, we observe that the peak amplitude scaling as a function of magnitude is penalized for strain rate (Figure S2a) rather than time integrated quantities (Figure S2c). Furthermore, the Ps wave always anticipates the amplitude content of the S waves (Figure S2b, Figure S2d).

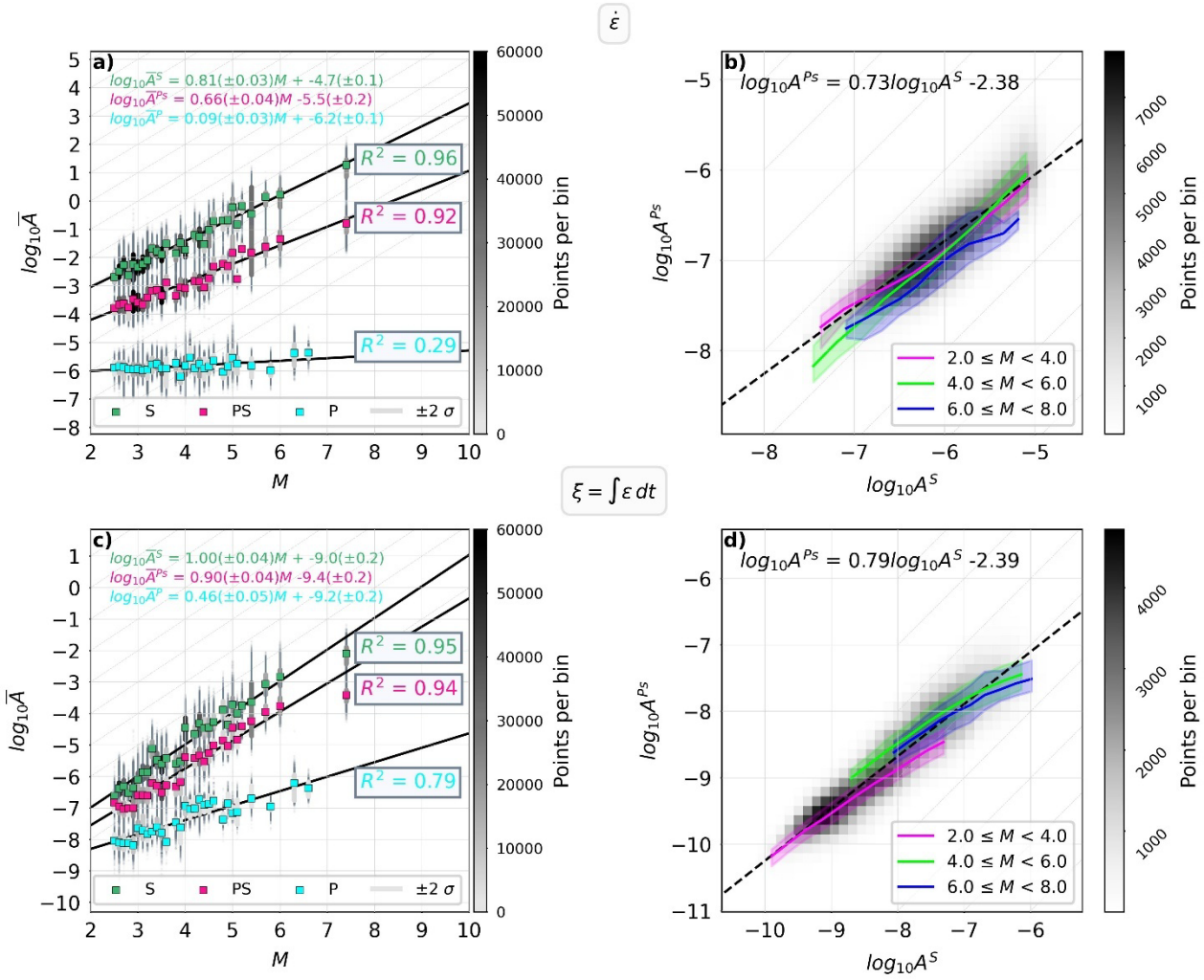

Figure S2. Representation of rescaled peak amplitudes as a function of magnitude, same as in Figure 2 of the main text, but for strain rate (a-b) and time integral of the strain (c-d).

We estimated the expected error due to the inversion of the linear relation that links earthquake magnitude to peak amplitude measurements. We repeated the analysis reported in Figure 2b of the main text also for the other two quantities, $\dot{\varepsilon}$ and ξ. We demonstrate that the use of strain rate peak amplitudes leads to larger errors in the estimation of magnitudes, as compared to displacement (Figure 2b). Indeed, the use of time integrated measurements such as ξ would lead to accurate magnitude estimates, almost equivalent to displacement. However, for operational reasons, using displacement or raw strain rate data may be more relevant than the strain time integral. Both displacement and time integral strain measurements involve spatial and/or temporal integration along the fiber. Impulsive instrumental noise or locally decoupled cable sections can

pollute these integrated measurements and necessitate the use of beforehand filters, which can reduce the bandwidth available for analysis. Here, the use of displacement is a good compromise, as in practice the data are streamed in velocity, and can be used in conjunction with onshore velocimetric stations.

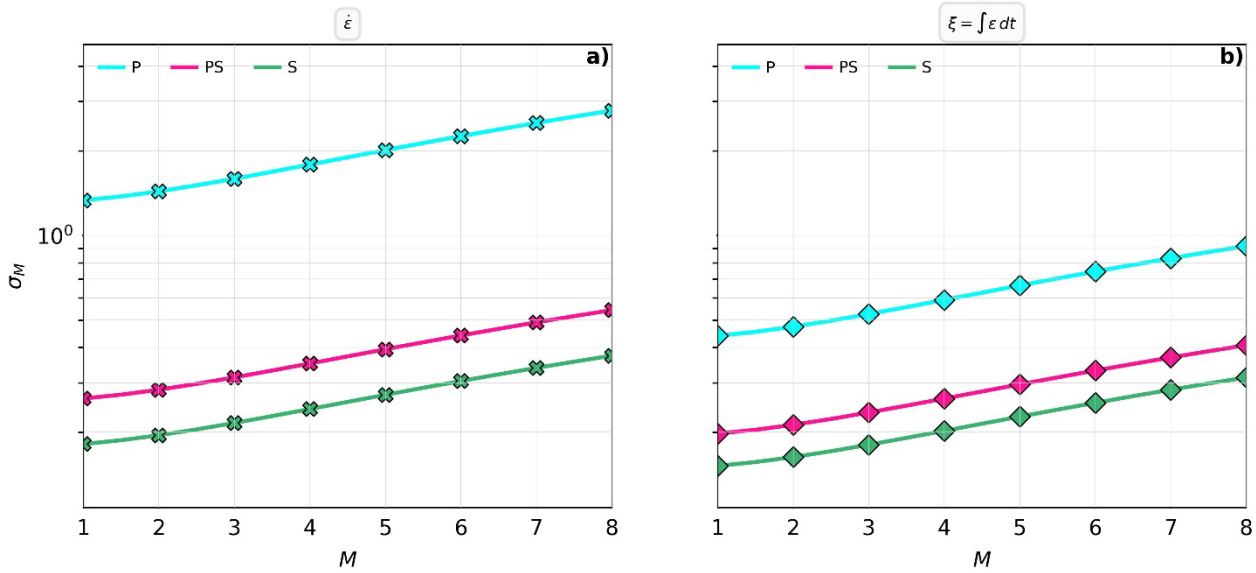

Figure S3. Expected error on magnitude prediction as a function of earthquake magnitude for the strain rate $\dot{\varepsilon}$ (a) and the time integral of the strain ξ (b).

S4

Here we represent, in three separated plots, the scaling relationships between peak amplitudes of Ps amplitudes estimated within time windows of $2s$, $4s$, and $6s$ from the observed arrival times, and earthquake magnitude. Figure S4 reproduces the results of Figure 4 in the main text, adding the information of single channel measurements in each of the three subplots.

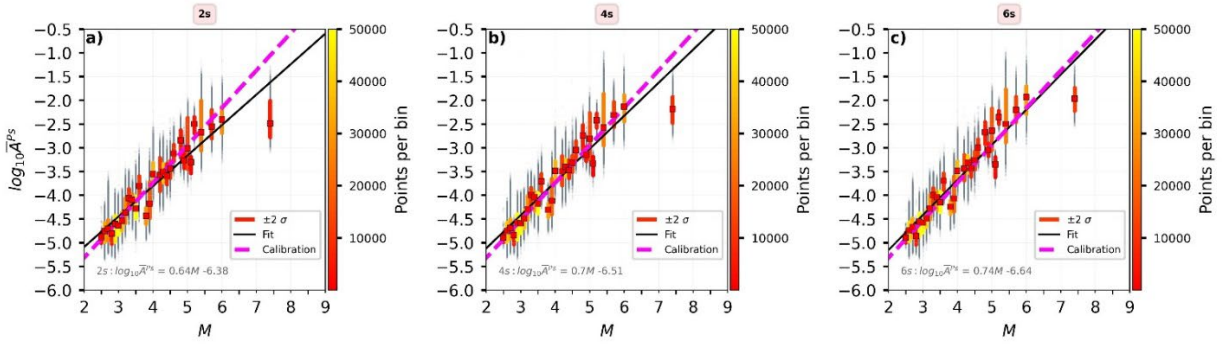

Figure S4. Rescaled peak amplitude as a function of magnitude for $2s$, $4s$ and $6s$ (a-c) time windows. Markers represent the binned amplitude values for each magnitude bin, while the grey dots in the background represent single channel estimates; the dashed pink line indicates the reference scaling as shown in Figure 2, obtained by tailoring the time windows and frequency band on the single events.

S4

As shown in main text Figure 4, the use of Ps amplitudes enables rapid assessment of earthquake magnitude from first seconds of DAS recording, even before S waves propagate along the cable. Here we add one more example of playbacks of real time magnitude estimation for a smaller magnitude event occurring closer to the array. Figure S5 reproduces the analysis for a $M4.2$ event occurring at a minimum hypocentral distance of 65 km from CCN.N, and that does not exhibit any saturation for the S wave. In this case, we also show how the magnitude estimates benefit from the inclusion of S wave amplitudes.

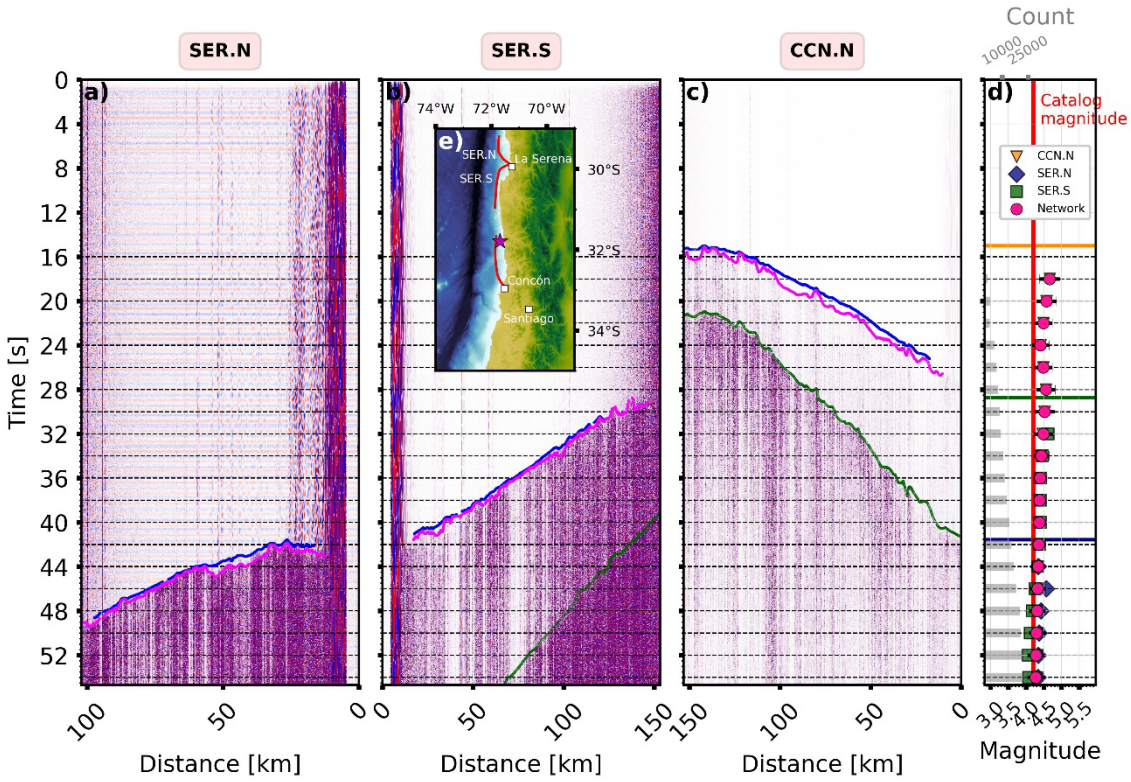

Figure S5. Magnitude estimation using Ps peak amplitudes for a M4.2 event occurred on 2024-09-23 between the cables of SER.N, SER.S and CCN.N. Panels (a)-(c) shows the strain rate trace high-pass filtered above 0.075Hz for the cables SER.N, SER.S, and CCN.N respectively, while the blue, pink, and green markers represent the P, Ps, and S arrival times. Panel (d) describes the magnitude estimation as a function of time, changing as new information is included, and compared with the catalog magnitude (vertical red line). The colored markers are the median estimation at each cable, while the pink circles depict the

median estimation obtained merging all the available information from the whole network, and the error bars represent the Standard Median Absolute Deviation (SMAD) of the magnitude distribution. Finally, the grey bars account for the number of points composing the magnitude distribution at each time step of the computation. Finally, panel (e) displays the geometry of the network (three red curves) and the earthquake epicenter location.

S5

When estimating peak amplitudes to calibrate scaling laws, we ensured to properly bandpass filter based on earthquake magnitude, to capture the low frequency plateau level of each event. Also, the time window duration was tailored to capture the whole source time function. Here in TableS1 we show the window duration and frequency bands adopted for the filtering.

Magnitude	Time window duration	Frequency band
$M < 3$	$2.0s$	$[1 - 20]Hz$
$3 \leq M < 4$	$2.0s$	$[0.5 - 10]Hz$
$4 \leq M < 5$	$3.0s$	$[0.1 - 5]Hz$
$5 \leq M < 6$	$10.0s$	$[0.02 - 2]Hz$
$M \geq 6$	$30.0s$	$[0.01 - 1]Hz$

Table S1. Time duration and frequency band selection used for the measurements of peak amplitudes, based on earthquake magnitude. The intervals are chosen based on the expected corner frequency-seismic moment distribution assuming self-similar characteristics.

S6

To correlate peak amplitudes to earthquake magnitude we characterized the contribution of propagation. We fitted the observed amplitude decay with hypocentral distance for each of the three seismic phases analyzed in this study (P, Ps, and S wave). In Figure S7, we plot the peak amplitudes, color-coded with earthquake magnitude, as a function of the hypocentral distance, along with black dashed lines indicating the attenuation curves obtained from the fit.

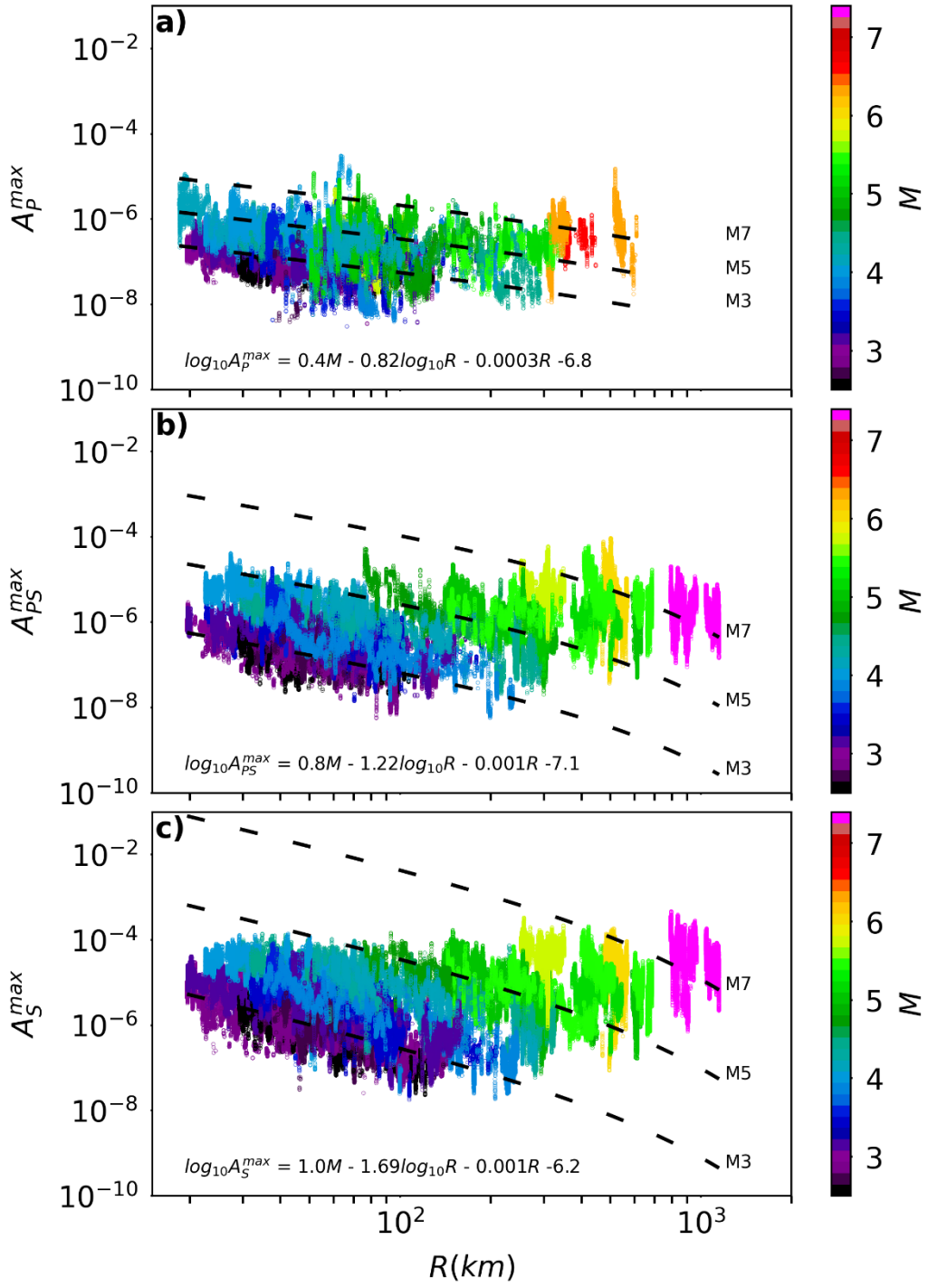

Figure S6. Peak amplitude decay with distance for P, Ps, S waves (a-b). Each dot represents peak displacement amplitudes, color coded based on earthquakes magnitude.

S7

As described in the methods section, we estimated the site-dependent residuals along the three fiber optic cables and used them to correct our peak amplitude measurements. Here we show the

variability of these residuals for the three seismic phases along each cable of the array.

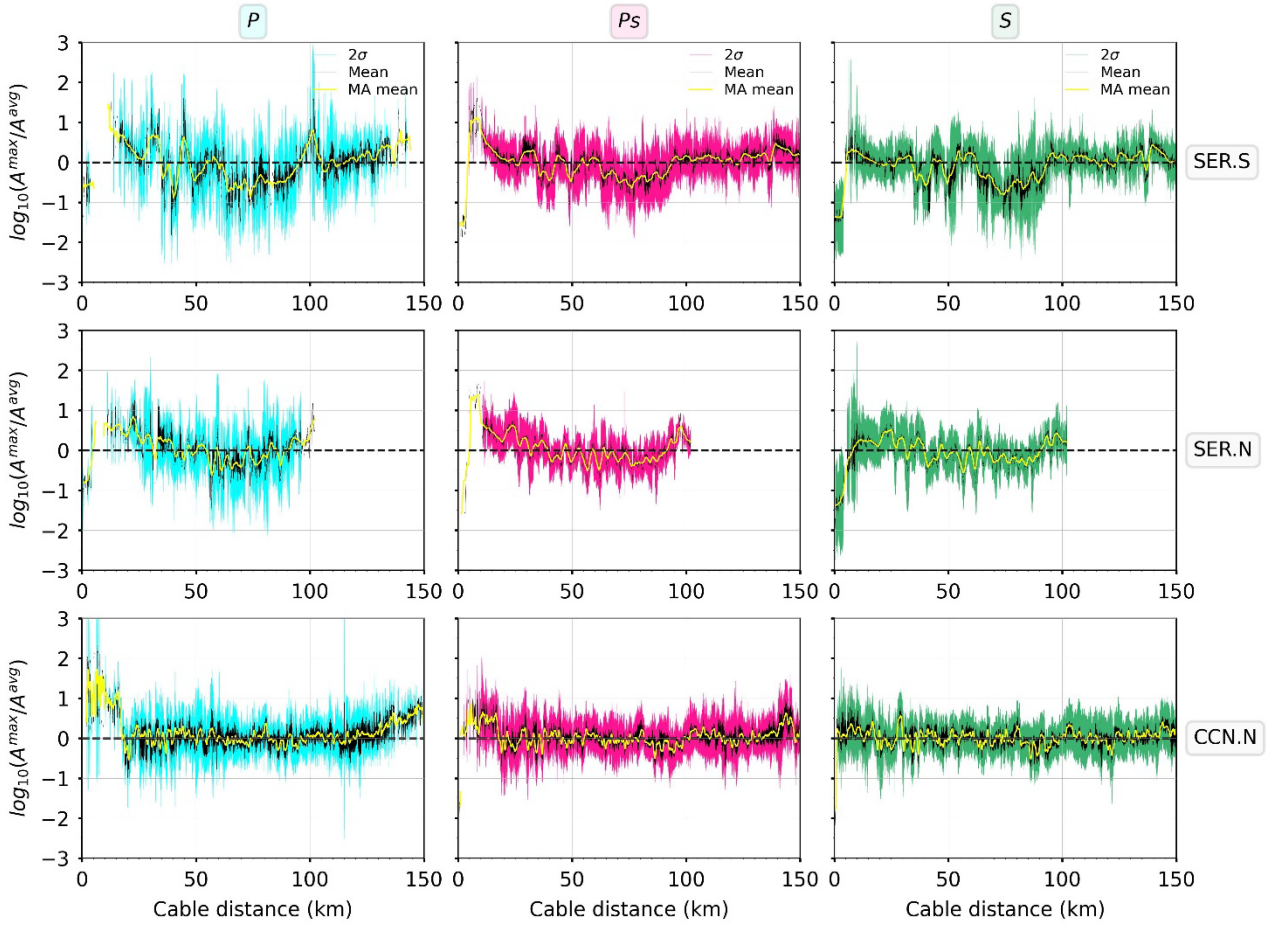

Figure S7. Average residuals as a function of distance along the cables for the whole ABYSS network. The black lines represent the average value of residual at each channel, while the yellow lines are obtained through a moving average of the black curves. The shaded areas represent the residuals variability, in terms of standard deviation, between all the events recorded at each cable.

Also, we related the amplitude residuals along the cables with the time delay between P and Ps waves shown in Figure S1. In Figure S8 we represent the time delays for the three cables, after subtracting the mean and normalizing between -1 and 1, as a function of distance along the fibers, and on the second axis we report the normalized amplitude residuals for Ps waves as a function of the distance along the DAS arrays.

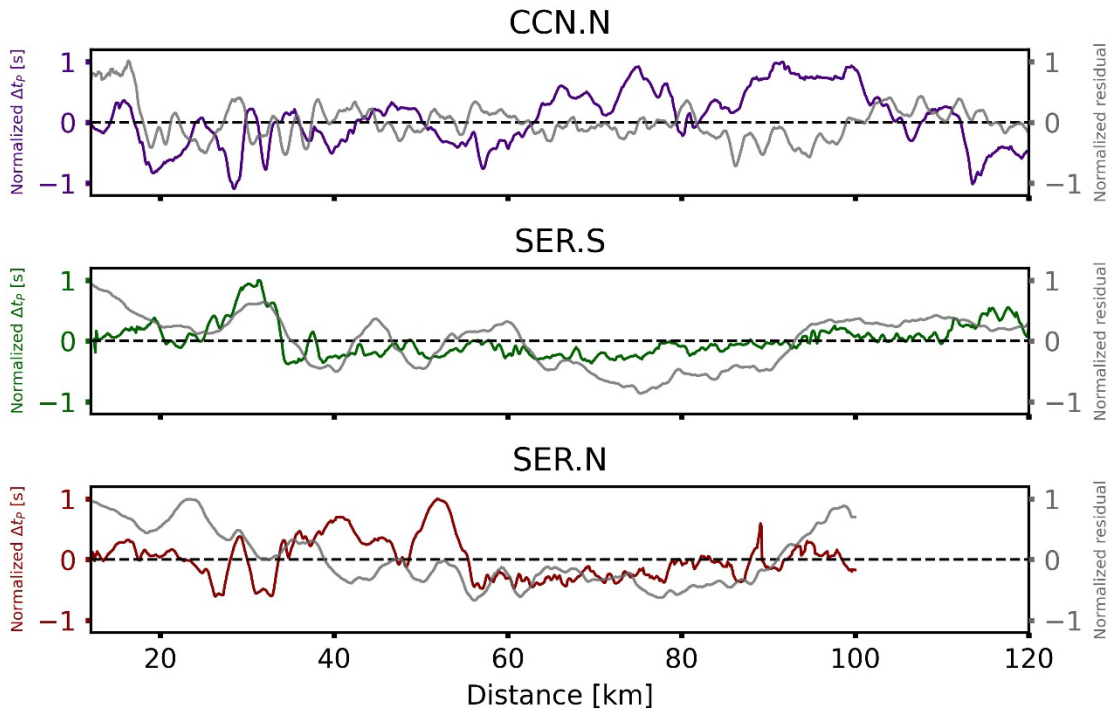

Figure S8. Normalized delays between P and Ps waves for the three cables (left axes) as a function of distance. Right axes describe the normalized amplitude residuals (as in Figure S7) but normalized between -1 and 1.

S8

Here we report the parameters used for evaluating the saturation threshold as a function of hypocentral distance for the ABYSS network.

Parameter	**CCN.N / SER.S**	**SER.N**
Laser wavelength λ	$1550 \times 10^{-9} m$	$1550 \times 10^{-9} m$
Fiber refractive index n	1.44	1.44
Photo-elastic coeff. ξ	0.79	0.79
Gauge length G_L	$30.64 m$	$30.64 m$
Time sampling Δt	$0.016 s$	$0.01 s$

Central frequency f_0	$1Hz$	$1Hz$
Wave velocity S wave	$3000\ m/s$	$3000\ m/s$
Wave velocity P wave	$5200\ m/s$	$5200\ m/s$

Table S2 Characteristic parameters used to estimate the maximum observable displacement.